# Enhanced Photocatalytic Activity and Mechanism of $La^{3+}$- Doped $BiPO_4$

Yulian Quan

Department of Environmental Engineering, Environmental Management College of China, Qinhuangdao, 066102, China

email: quanyulian@126.com

**Keywords:** Bismuth Phosphate; Lanthanum; Photocatalytic activity; Methylene Blue

**Abstract.** $La^{3+}$- doped $BiPO_4$ photocatalysts were synthesized by a hydrothermal method. The morphologies, structures, components, and light absorption properties of the photocatalysts were evaluated using XRD, FESEM, EDX, BET, XPS, and DRS techniques. La-doping could improve the photocatalytic activity of $BiPO_4$ for degrading methylene blue under ultraviolet irradiation, The apparent reaction rate of $La^{3+}$-$BiPO_4$ was 0.31min$^{-1}$, which was 3.4 times higher than that of pure $BiPO_4$. The outstanding photocatalytic activity could be mainly attributed to the higher valence band position and more effective electron-hole pair separation, ensured by Mott-Schottky and EIS test. Moreover, radical scavenger experiments confirmed that holes constituted the active species.

## Introduction

Photocatalysis has attracted tremendous attention because of its great potential in renewable energy and environmental protection [1][2]. Among the numerous semiconductor photocatalysts, the novel $BiPO_4$ has proven to be a suitable alternative to $TiO_2$[3], and is frequently investigated owing to its low cost and significant photocatalytic oxidative ability in the decomposition of organic dyes and other pollutants [4][5]. Nevertheless, widespread applications of $BiPO_4$ have been hindered by its large grain size and weak response to visible light [3][6]. Therefore, it is necessary to identify effective approaches to enhance the photocatalytic activity of $BiPO_4$. In addition, systemic studies regarding the mechanism and pathway of photogenerated electron-hole pairs ($e^-/h^+$) under irradiation should be conducted in order to design efficient doped photocatalysts, which will promote practical applications in areas such as environmental protection.

A significant amount of work has been carried out in an effort to enhance the photocatalytic activity of $BiPO_4$, such as improving preparation methods [6], modificating with noble metals [7], and fabricating heterojunctions [8]. It was also reported that doping with F and Ag could enhance the photocatalytic activity of $BiPO_4$ [9][10]. The effects of lanthanide doping on the photocatalytic activity of $BiPO_4$ have not been reported, to the best of our knowledge. Other research has shown that lanthanide ions were good dopants for $TiO_2$ and $BiVO_4$ [11][12], owing to their 4f electron configuration. Among lanthanide elements, La is attractive because it is cheap and can reduce the recombination rate of $e^-/h^+$ effectively. Therefore, doping with $La^{3+}$ may be an effective method to enhance the photocatalytic activity of $BiPO_4$.

In this study, lanthanum ion-doped $BiPO_4$ spherical particles were fabricated by a simple hydrothermal process. The crystal structure, optical properties, and photo-electrochemical performance of $La^{3+}$-$BiPO_4$ catalysts were measured. Their photocatalytic activities were evaluated in the decomposition of methylene blue (MB) under ultraviolet (UV) light. Furthermore, the possible mechanism behind the improved photocatalytic properties of $La^{3+}$-$BiPO_4$ was investigated on the basis of its energy band structure and the measurement of reactive species.

 

## Experimental

Synthesis of $La^{3+}$-$BiPO_4$ photocatalysts

All analytically pure reagents were provided by Sinopharm Chemical Reagent Company. Briefly, appropriate amounts of $Bi(NO_3)_3$•$5H_2O$ and $La(NO_3)_3 \cdot 6H_2O$ were added to 29 mL of a nitric acid solution (26.4 mL distilled water + 2.6 mL $HNO_3$), into which 1 mL of tri-butyl-phosphate (TBP) was added drop-wise. The mixed solution was subsequently stirred for 0.5 h. The pH was maintained at less than 1. The resulting suspension was transferred into a Teflon-lined stainless steel autoclave and maintained at 200℃ for 3 h. The final product was filtered and washed 3 times with distilled water and ethanol, and then dried at 80℃ for 12 h. $La^{3+}$-$BiPO_4$ catalysts with 2% La contents (mol fraction) were synthesized using the aforementioned method.

Characterization of photocatalysts

The obtained catalysts were examined by X-ray diffraction (XRD) (Dmax-2500, Rigaku, Japan) with Cu-Kα radiation (λ = 0.15406nm) at 40 kV and 200 mA. Field emission scanning electron microscopy (FE-SEM) images and EDX spectra were collected using a scanning electron microscope (Supera 55, Zeiss, German) with a scanning voltage of 10.00 kV. The elemental compositions and valence states of the samples were analyzed using X-ray photoelectron spectroscopy (XPS) (ESCALAB 210, VG, UK), using a non-monochromatic Mg Kα X-ray source (300 W). The Brunauer-Emmett-Teller (BET) specific surface area was determined by a surface area analyzer (ASAP 2020 HD88, Micromeritics, USA). Diffuse reflectance spectra (DRS) were measured using a UV-vis spectrophotometer (UV-4100, Hitachi, Japan) equipped with an integrating sphere attachment.

Evaluation of photocatalytic activity

The photocatalytic activities were investigated in the degradation of MB under UV irradiation. A 20 W germicidal lamp (λ = 254 nm) was used as irradiation source. The average light intensity of the lamp was 18.2 uw/$cm^2$. Before irradiation, a MB solution (250 mL, $2\times10^{-5}$ mol/L) containing 0.125g catalysts was stirred for 30 min in the dark in order to establish the adsorption-desorption equilibrium between MB and the catalysts. Aliquots (5 mL) of the reaction solution were sampled in specified time intervals and were centrifuged (10000 rpm, 10 min) to remove the catalysts particles. The absorbance of MB (the maximum absorption peak occurs at 664 nm) was recorded using a UV-Vis spectrophotometer (TU-1810D, Beijing Purkinje General Instrument Co., Ltd.). The radical and hole trapping experiments were similar to the above-mentioned photodegradation experiment. The scavengers, tert-butyl alcohol (t-BuOH) and ethylenediaminetetraacetic acid disodium salt (EDTA-2Na), were added to the reaction solution prior to the addition of the photocatalysts.

Photoelectrochemical measurements

Photoelectrochemical measurements were carried out using an electrochemical system (Priceton Parstat-4000, USA). A $La^{3+}$-$BiPO_4$ film was deposited on ITO conducting glass ($La^{3+}$-$BiPO_4$@ITO). UV irradiation was executed using a 20 W ultraviolet germicidal lamp (Foshan electric lighting co., Ltd.). A standard three electrode cell with a $La^{3+}$-$BiPO_4$@ITO film as the working electrode, standard Ag/AgCl electrode as the reference electrode, and platinum wire as the counter electrode was used in the photoelectrochemical measurements. $Na_2SO_4$ (0.1 mol/L) was used as the electrolyte solution.

## Results and discussion

Characterization

Fig. 1 presents the XRD patterns of $La^{3+}$-$BiPO_4$. The main diffraction peaks coincided with the monoclinic phase of $BiPO_4$ (JCPDS No. 80-0209) and no peaks from crystals containing La could be detected due to the small doping amount. Therefore, it was concluded that $La^{3+}$ was doped into the crystal lattice. The EDX spectra of pure $BiPO_4$ and $La^{3+}$-$BiPO_4$ are shown in Fig. 2. The ratio of Bi, P, and O was identical to the expected stoichiometry in pure $BiPO_4$. For $La^{3+}$-$BiPO_4$, the appearance of the La peak demonstrated the coexistence of La and $BiPO_4$ in the final product.

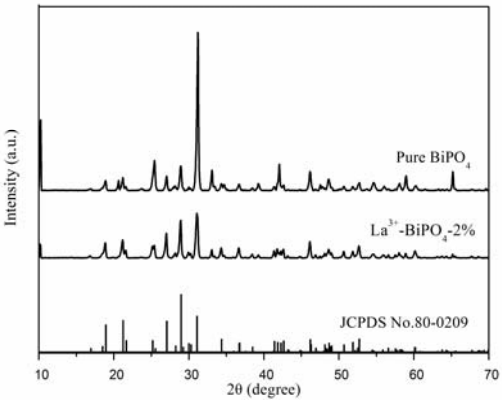


Fig.1. XRD patterns of different catalysts

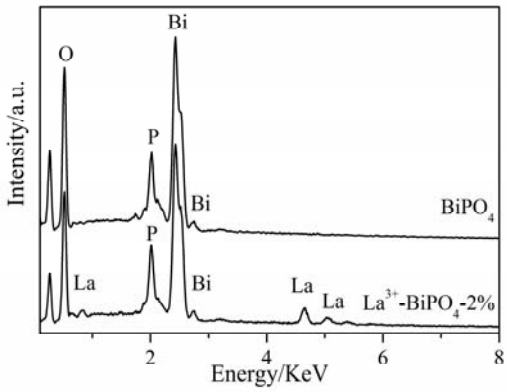


Fig.2.EDX images of different catalysts

Fig. 3 shows the SEM images of pure $BiPO_4$ and $La^{3+}$-$BiPO_4$. $BiPO_4$ agglomerated into irregular nanorods with diameters of 180-220 nm and lengths of 0.3-1.0 μm. The morphology of $La^{3+}$-$BiPO_4$ was different from that of pure $BiPO_4$. It was composed of spherical particles and some irregularly shaped aggregates. The diameters of the spherical particles ranged from 80 to 150 nm. Doping with $La^{3+}$ inhibited the growth and agglomeration of the nanorods to a certain extent. Therefore, the BET surface area of $La^{3+}$-$BiPO_4$ (3.37 $m^2/g$) was greater than that of $BiPO_4$ (2.93 $m^2/g$). These would lead to an increased number of active sites and would benefit the photocatalytic reaction.

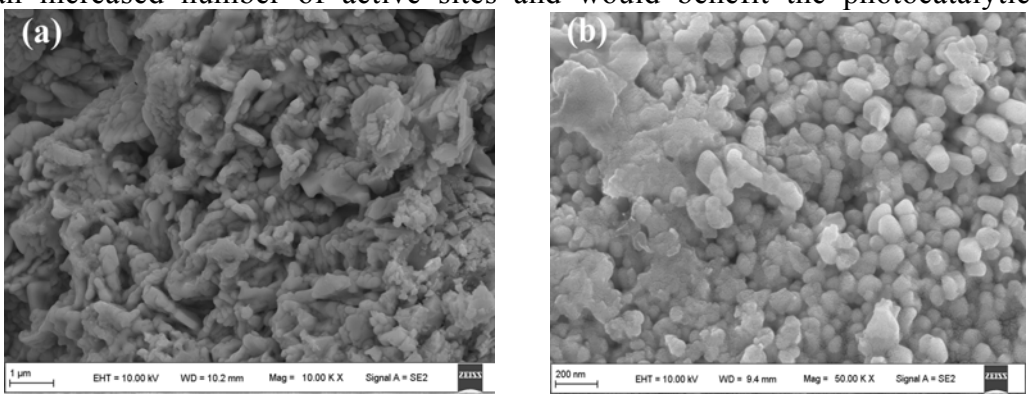


Fig.3. SEM images of different $BiPO_4$ powders:（a）$BiPO_4$;（b）$La^{3+}$-$BiPO_4$-2%

Fig. 4 shows the XPS spectra of the samples. The peaks at 159.87 eV, 165.18 eV and 161.95 eV, 167.29 eV corresponded to Bi 4f 7/2 and Bi 4f 5/2 binding energies for $Bi^{3+}$ in $BiPO_4$ and $La^{3+}$-$BiPO_4$ respectively. The binding energies of P 2p were 133.30 eV and 135.30 eV, attributed to P of $PO_4^{3-}$. The peaks located at 531.16 eV and 533.24 eV were indexed to O 1s, and were associated with the lattice oxygen of $BiPO_4$. The oxygen content was increased by 3% after doping. While La entered the lattice of $BiPO_4$, the lattice expansion facilitated the escape of the oxygen atoms from the lattice to produce oxygen vacancies [13], thereby increasing the adsorption of oxygen. Oxygen vacancies could be used as capture agents and increase the separation of electron-hole pair [14]. The peaks located at 840.71 eV and 854.51 eV corresponded to La 3d 3/2 and La 3d 5/2 in $La^{3+}$-$BiPO_4$, respectively. These results suggested the presence of trivalent La. The

satellite peak of La 3d5/2 was at 838.1 eV, which was attributed to the bonding in the lanthanum oxide clusters [15].

The typical DRS of pure $BiPO_4$ and $La^{3+}$-$BiPO_4$ are presented in Fig. 5. The samples absorbed light mainly in the ultraviolet band. The absorption edge shifted slightly towards the ultraviolet band for $La^{3+}$-$BiPO_4$. This may be associated with the introduction of $La_2O_3$ and a similar result has also been reported in La-doped ZnO by S. Anandan et al. [15]. A blue shift would lead to a marginal decrease in the spectral response, but the increase in light absorption from 200nm to 260nm might improve its catalytic activity under ultraviolet light. The band gaps ($E_g$) of pure $BiPO_4$ and $La^{3+}$-$BiPO_4$ were estimated to be 3.32 eV and 3.80 eV, respectively, on the basis of Tauc's equation [16]. Therefore, the blue shift was attributed to the increased bandgap of $La^{3+}$-$BiPO_4$, which was associated with the lattice distortion. This assumption was consistent with XRD and SEM results, in which La dopants impacted the crystallization process and resulted in a decrease in the grain size.

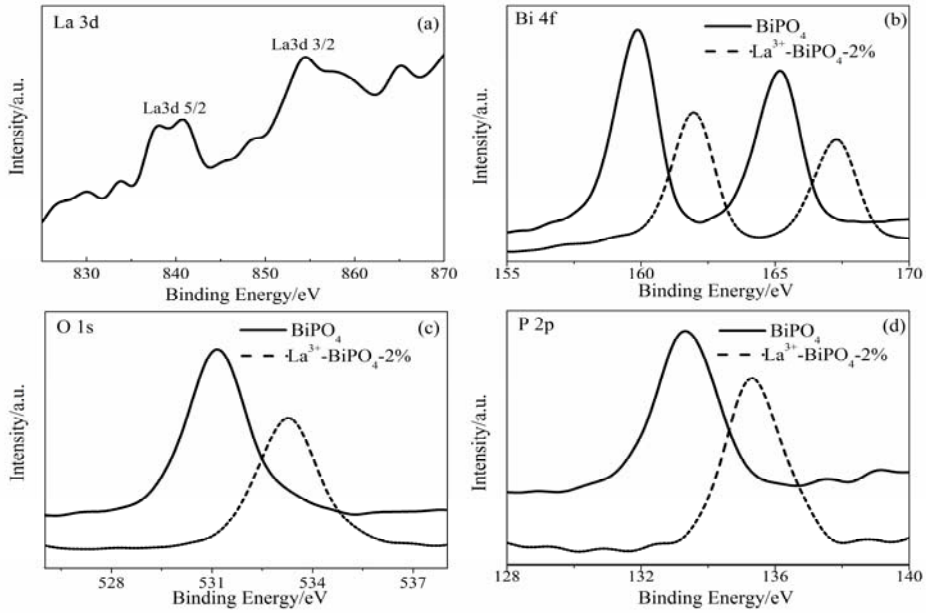


Fig.4. XPS survey spectrum of different catalysts

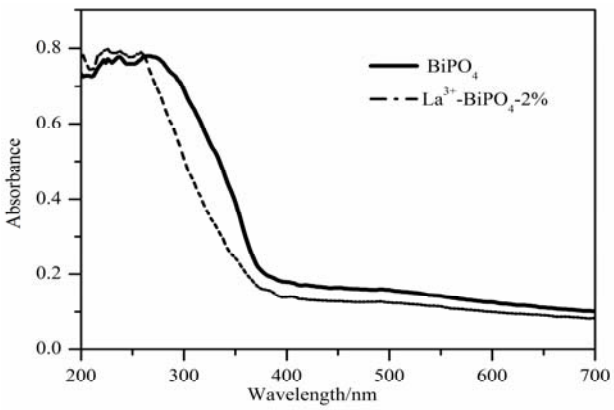


Fig.5. DRS spectra of different catalysts

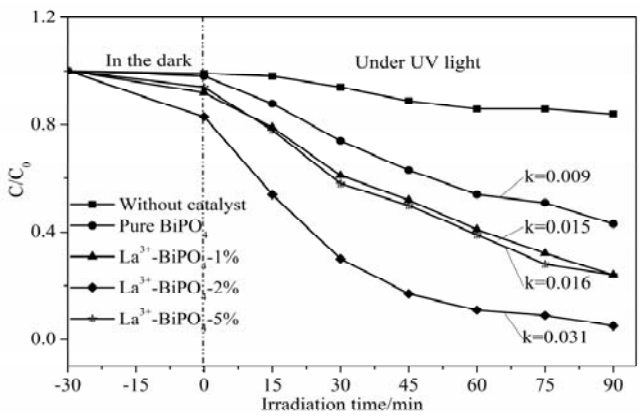


Fig.6. Photocatalytic activities of different catalysts

Photocatalytic activity

The variation in the relative concentration of MB with irradiation time is shown in Fig. 6. For comparison, MB photolysis was also conducted in the blank experiment. The removal rate of MB was slow (about 15%) in the absence of a photocatalyst under ultraviolet illumination. After 90 min of irradiation, the MB degradation percentage was about 95% and 56% for $La^{3+}$-$BiPO_4$ and pure $BiPO_4$, respectively. The results demonstrated that lanthanide doping could enhance the photocatalytic performance of $BiPO_4$ in the decomposition of MB.

The degradation rates of MB over the samples were calculated according to the following apparent pseudo-first-order kinetics equation[7]. The apparent reaction rate of $La^{3+}$-$BiPO_4$ was $0.31min^{-1}$, which was 3.4 times higher than that of pure $BiPO_4$, which further confirmed the activity enhancement of $La^{3+}$-$BiPO_4$. Besides, the photocatalytic activities of the other $La^{3+}$-$BiPO_4$ samples with 1% and 5% La doping amounts were measured. The corresponding apparent reaction rates were calculated to be 0.009, 0.015, 0.031, $0.016min^{-1}$ for pure $BiPO_4$, $La^{3+}$-$BiPO_4$-1%, $La^{3+}$-$BiPO_4$-2%, and $La^{3+}$-$BiPO_4$-5%.The above results ensured the best activity of $La^{3+}$-$BiPO_4$-2%.

Identification of the active species

In order to elucidate the photocatalytic mechanism in the reaction process, we tested the main oxidative species by radical and hole trapping experiments. The experiments were conducted by adding the hydroxyl radical scavenger tBuOH and the hole scavenger EDTA-2Na [17]. As shown in Fig. 7, the photodegradation rates of MB with $BiPO_4$ and $La^{3+}$-$BiPO_4$ were both suppressed by the addition of two scavengers, but were greatly inhibited by the hole scavenger. It was concluded that photogenerated holes and hydroxyl radicals were the active species during the photocatalysis, while the former predominated in oxidizing adsorbed organic pollutants. This was consistent with some literature reports [7].

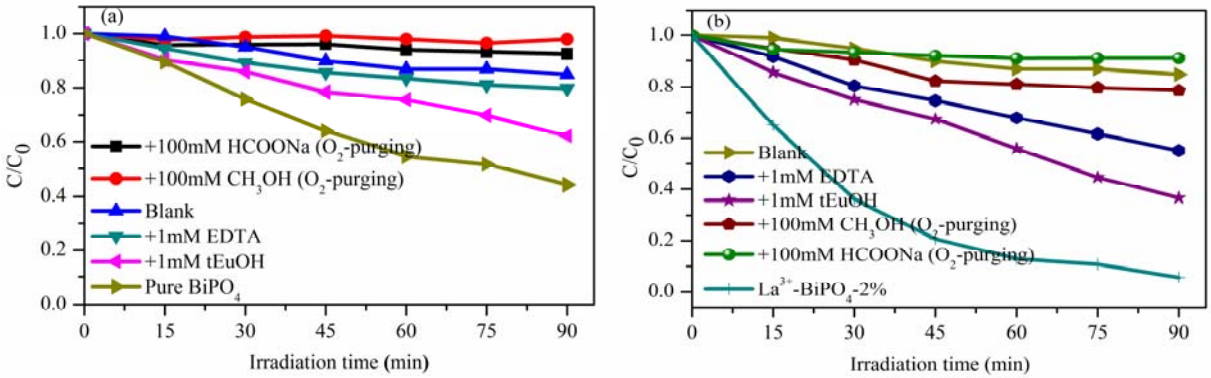


Fig.7. The plots of photogenerated carrier trapping in the photodegradation of MB by (a) pure $BiPO_4$ and (b) $La^{3+}$-$BiPO_4$-2% under UV irradiation.

Meanwhile, $HO_2$•/$O_2^-$• may also be used as active species in other photocatalytic reactions. When oxygen was bubbled into the reaction system, most •OH radicals became $HO_2$•/$O_2^-$• when they coexisted with 100 mM methanol or formate [18]. Accordingly, if $HO_2$•/$O_2^-$• is assumed to be a powerful oxidant for the photodegradation of MB, the concentration of MB would decrease greatly due to methanol or formate. However, Fig. 7 suggested otherwise. Therefore, $HO_2$•/$O_2^-$• was not the main active species and •OH radicals played significant roles in the $BiPO_4$ photocatalytic system.

Mechanism of enhanced photoactivity

Photocatalytic activity enhancement of $La^{3+}$-$BiPO_4$ is related to surface area, oxidation abilities of photogenerated holes, as well as migration and separation efficiency of the carriers. The SEM results indicated that doping with $La^{3+}$ inhibited the growth of the crystals to a certain extent. The BET surface area of $La^{3+}$-$BiPO_4$-2% was greater than that of $BiPO_4$. These would lead to an increased number of active sites and would benefit the photocatalytic reaction.

To identify the oxidation abilities of photogenerated holes, the valence band position ($E_{VB}$) was calculated using the conductive band position ($E_{CB}$) and the band gap ($E_{VB}$=$E_{CB}$ + $E_g$). The difference between the $E_{CB}$ and flat band potential ($E_{FB}$) is assumed to be -0.3 V ($E_{CB}$ = -0.3 V + $E_{FB}$) in n-typed semiconductors [19]. The $E_{FB}$ of $La^{3+}$-$BiPO_4$ and $BiPO_4$ were -0.69 V and -0.64 V (vs Ag/AgCl), as shown in Fig. 8. Therefore, the $E_{CB}$ were -0.99 V and -0.94 V (vs Ag/AgCl) , respectively. According to Ag/AgCl vs NHE= 0.2224 V, the $E_{CB}$ of $La^{3+}$-$BiPO_4$ and $BiPO_4$ were -0.77 V and -0.72V vs. NHE. Combined with the band gap, the $E_{VB}$ of $La^{3+}$-$BiPO_4$-2% and $BiPO_4$ were estimated to be +3.03V and +2.60V vs NHE. It was suggested that the $E_{VB}$ of $La^{3+}$-$BiPO_4$ was greater than that of $BiPO_4$, which may enhance the oxidation abilities of photogenerated holes and facilitate the production of hydroxyl radicals. Furthermore, the photogenerated holes were the main

active species with $La^{3+}$-$BiPO_4$, as discussed above. As such, it is reasonable that the photocatalytic activity of $La^{3+}$-$BiPO_4$ is much greater than that of $BiPO_4$.

As shown in Fig. 9, the transfer and separation efficiency of the photogenerated $e^-/h^+$ was described by electrochemical impedance spectroscopy (EIS). The smaller the diameters of the EIS Nyquist plots, the better separation of electrons and holes in the electrode-electrolyte interface region [20]. The diameter of the $La^{3+}$-$BiPO_4$semicircle was smaller than that of $BiPO_4$. This implied that doping with $La^{3+}$ caused a low $e^-/h^+$ recombination rate. After doping with $La^{3+}$, the lattice distortion might produce oxygen vacancies ($Vo^+$) [13], which could be used as capture agents and increase the separation of $e^-/h^+$ [14]. As such, $La^{3+}$-$BiPO_4$-2% showed a better photocatalytic activity than $BiPO_4$. In view of the above discussion, a possible photodegradation mechanism of MB with $La^{3+}$-$BiPO_4$ is presented in Fig. 10.

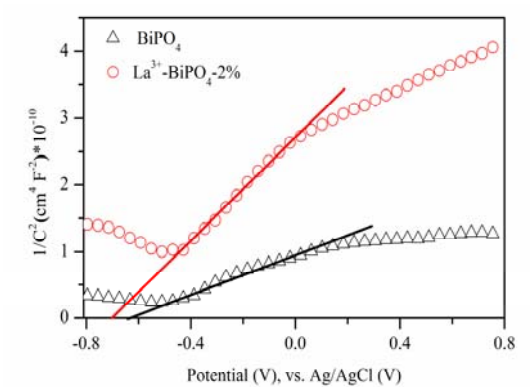


Fig.8. Mott-Schottky plots for different catalysts. Frequency: 1 kHz

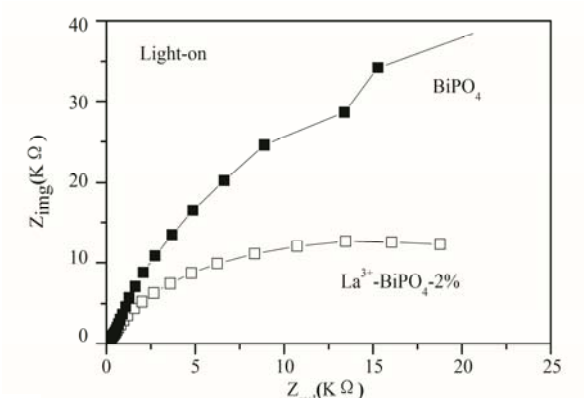


Fig.9. EIS spectra of different catalysts

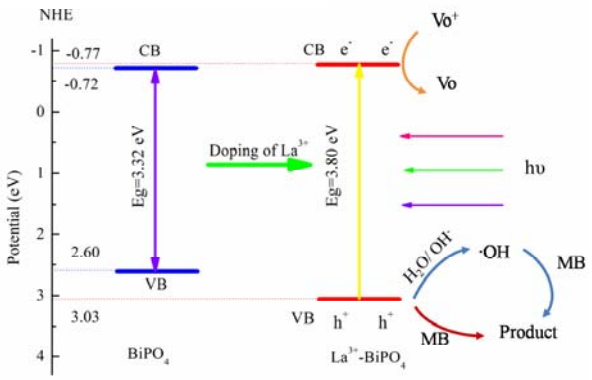


Fig.10. Schematic illustration for the photocatalytic mechanism of $La^{3+}$-$BiPO_4$

## Conclusion

In conclusion, $La^{3+}$-doped $BiPO_4$ nano spherical particles were fabricated via a hydrothermal method. $La^{3+}$-$BiPO_4$ exhibited superior catalytic activity than $BiPO_4$ in the decomposition of MB under UV irradiation. Photogenerated holes were found to be the main active species in the photocatalytic reaction. Photocatalytic activity enhancement of $La^{3+}$-$BiPO_4$ was attributed to its smaller size and larger surface area, particularly the quickly transfer and separation rate of the photogenerated $e^-/h^+$ and the high potential of the photogenerated holes.


## Acknowledgement

This study was subsidized by the Natural Science Foundation of the Educational Committee of Hebei Province (Project No.QN20131032).

## References


[1] Hoffmann M R, Martin S T, Choi W, et al. Environmental applications of semiconductor photocatalysis [J]. Chemical Reviews, 1995 (95) 69–96.

[2] Chen X, Mao S S. Titanium dioxide nanomaterials: Synthesis, properties, modifications, and applications [J]. Chemical Reviews, 2007 (107) 2891–2959.

[3] Pan C S, Zhu Y F. New type of $BiPO_4$ oxy-acid salt photocatalyst with high photocatalytic activity on degradation of dye [J]. Environmental Science & Technology, 2010 (44) 5570-5574.

[4] Zhang Y F, Selvarajb R, Sillanpääa M, et al. The influence of operating parameters on heterogeneous photocatalytic mineralization of phenol over $BiPO_4$ [J]. Chemical Engineering Journal, 2014 (245) 117-123.

[5] Xu J, Li L, Guo C, et al. Photocatalytic degradation of carbamazepine by tailored $BiPO_4$: efficiency, intermediates and pathway [J]. Applied Catalysis B, 2013 (130-131) 285-292.

[6] Nithya VD, Hanitha B, Surendran S, et al. Effect of pH on the sonochemical synthesis of $BiPO_4$ nanostructures and its electrochemical properties for pseudocapacitors [J]. Ultrasonics Sonochemistry, 2015 (22) 300-310.

[7] Zhang Y A, Fan H Q, Li M M, et al. Ag/$BiPO_4$ heterostructures: synthesis, characterization and their enhanced photocatalytic properties [J]. Dalton Transactions, 2013 (42) 13172-13178.

[8] Wu S Y, Zhang H, Lian Y W, et al. Preparation, characterization and enhanced visible-light photocatalytic activities of $BiPO_4$/$BiVO_4$ composites [J]. Materials Research Bulletin, 2013 (48) 2901-2907.

[9] Liu Y F, Lv Y H, Zhu Y Y, et al. Fluorine mediated photocatalytic activity of $BiPO_4$ [J]. Applied Catalysis B, 2014 (147) 851-857.

[10] Fulekar M H, Singh A, Dutta D P, et al. Ag incorporated nano $BiPO_4$: sonochemical synthesis, characterization and improved visible light photocatalytic properties [J]. RSC Advances, 2014 (4) 10097-10107.

[11] Jing L Q, Sun X J, Xin B F, et al. The preparation and characterization of La doped $TiO_2$ nanoparticles and their photocatalytic activity [J]. Journal of Solid State Chemistry, 2004 (177) 3375-3382.

[12] Wang M, Che Y S, Niu C, et al. Lanthanum and boron co-doped $BiVO_4$ with enhanced visible light photocatalytic activity for degradation of methyl orange [J]. Journal of Rare Earths, 2013 (31) 878-884.

[13] Song H, Ozkan U S. Changing the oxygen mobility in Co/Ceria catalysts by Ca incorporation: implications for ethanol steam reforming [J]. Journal of Physical Chemistry A, 2010 (114) 3796-3801.

[14] Lv Y, Liu Y, Zhu Y, et al. Surface oxygen vacancy induced photocatalytic performance enhancement of a $BiPO_4$ nanorod [J]. J journal of Materials Chemistry A, 2014 (2) 1174-1182.

[15] Anandana S, Vinua A, Sheeja Lovelyb K L P, et al. Photocatalytic activity of La-doped ZnO for the degradation of monocrotophos in aqueous suspension [J]. Journal of Molecular Catalysis A , 2007 (266) 149-157.

[16] Tauc J, Grigorovici R, Vancu A. Optical properties and electronic structure of amorphous germanium [J]. Physical Status Solidi B, 1966 (15) 627–637.

[17] Zhou J, Deng C, Si S, et al. Study on the effect of EDTA on the photocatalytic reduction of

mercury onto nanocrystalline titania using quartz crystal microbalance and differential pulse voltammetry [J]. Electrochimica Acta, 2011 (56) 2062-2067.

[18] Yoon S H, Lee J H. Oxidation mechanism of As(III) in the UV/$TiO_2$ system: Evidence for a direct hole oxidation mechanism [J]. Environmental Science & Technology, 2005 (39) 9695-9701.

[19] Ogisu K, Ishikawa A, Shimodaira Y, et al. Electronic band structures and photochemical properties of La−Ga-based oxysulfides [J]. Journal of Physical Chemistry C, 2008 (112) 11978-11984.

[20] Hosseini Z, Taghavinia N, Sharifi N, et al. Fabrication of high conductivity $TiO_2$/Ag fibrous electrode by the electrophoretic deposition method [J]. Journal of Physical Chemistry C, 2008 (112) 18686 -18689.